EBioMedicine 42 (2019) 281–295

Contents lists available at ScienceDirect

EBioMedicine

journal homepage: www.ebiomedicine.com

EBioMedicine
Published by THE LANCET

Research paper

Simultaneous blocking of CD47 and PD-L1 increases innate and adaptive cancer immune responses and cytokine release

Shu Lian [a], Ruizhi Xie [a], Yuying Ye [b], Xiaodong Xie [a], Shuhui Li [a], Yusheng Lu [a,c], Bifei Li [a], Yunlong Cheng [a], Vladimir L. Katanaev [d,e], Lee Jia [a,c,*]

[a] Cancer Metastasis Alert and Prevention Center, College of Chemistry, Fujian Provincial Key Laboratory of Cancer Metastasis Chemoprevention and Chemotherapy, Fuzhou University, Fuzhou, China
[b] Fujian Provincial People's Hospital Affiliated to Fujian University of Traditional Chinese Medicine, Fuzhou 350004, China
[c] Marine Drug R&D Center, Institute of Oceangraphy, Minjiang University, Fuzhou 350108, China
[d] Translational Research Center in Oncohaematology, Department of Cell Physiology and Metabolism, Faculty of Medicine, University of Geneva, Switzerland
[e] Head of the Natural Products Drug Discovery Laboratory, School of Biomedicine, Far Eastern Federal University, Vladivostok, Russia

ARTICLE INFO

Article history:
Received 12 December 2018
Received in revised form 6 March 2019
Accepted 7 March 2019
Available online 14 March 2019

Keywords:
CD47/SIPR-α
PD-L1/PD-1
siRNA
Immune therapy
Liposome
Gene therapy
EpCAM targeted

ABSTRACT

Background: Treatment multiple tumors by immune therapy can be achieved by mobilizing both innate and adaptive immunity. The programmed death ligand 1 (PD-L1; or CD274, B7-H1) is a critical "don't find me" signal to the adaptive immune system. Equally CD47 is a critical "don't eat me" signal to the innate immune system and a regulator of the adaptive immune response.
Method: Both of CD47 and PD-L1 are overexpressed on the surface of cancer cells to enable to escape immune-surveillance. We designed EpCAM (epithelial cell adhesion molecule)-targeted cationic liposome (LPP-P4-Ep) containing si-CD47 and si-PD-L1 could target high-EpCAM cancer cells and knockdown both CD47 and PD-L1 proteins.
Findings: Efficient silencing of CD47 and PD-L1 versus single gene silencing in vivo by systemic administration of LPP-P4-Ep could significantly inhibited the growth of solid tumors in subcutaneous and reduced lung metastasis in lung metastasis model. Target delivery of the complexes LPP-P4-Ep increased anti-tumor T cell and NK cell response, and release various cytokines including IFN-γ and IL-6 in vivo and in vitro.
Interpretation: This multi-nanoparticles showed significantly high-EpCAM tumor targeting and lower toxicity, and enhanced immune therapeutic efficacy. Our data indicated that dual-blockade tumor cell-specific innate and adaptive checkpoints represents an improved strategy for tumor immunotherapy.
Fund: This research supported by the Ministry of Science and Technology of the People's Republic of China (grant number 2015CB931804); the National Natural Science Foundation of China (NSFC, grant numbers 81703555, U1505225 and 81773063), and the China Postdoctoral Science Foundation (grant number 2017 M620268).

1. Introduction

Cancer immunotherapy is now considered a pillar of cancer treatment, alongside surgery, chemotherapy, and radiation. The use of immunotherapy for cancer has become widespread in recent decades and is used to treat both solid and hematological malignances [1]. Recently emerging research targets include co-inhibitory and co-stimulatory markers of the innate and adaptive immune system [2]. Both the innate and adaptive immune system are critical to the efficacy of cytotoxic immune therapy [3,4].

PD-L1 (programmed death-ligand 1) is a member protein that is highly expressed on many tumor cells [5,6]. The programmed cell death protein 1 (PD-1), are receptors expressed on the surface of cytotoxic T-cells that interact with PD-L1 on APCs (antigen presenting cell), which helps the cancer cell evade T-cell-mediated death, and dampens anti-tumor adaptive immune responses. Immune checkpoint inhibitors prevent the receptors PD-1 and ligand PD-L1 from binding to each other, thereby disrupting signaling [7–9].

CD47, first identified as Integrin-Associated Protein (IAP) [10–13], is another cell-surface immunoglobulin that negatively regulates anti-tumor immunity through suppression of phagocytosis. CD47 transmits an inhibitory "don't eat me" signal upon ligation with its receptor signal regulatory protein α (SIRPα), which is expressed primarily on phagocytic cells, including monocytes, macrophages, dendritic cells and neutrophils [14,15]. CD47-SIRPα axis has been explored its essential role

* Corresponding author at: Cancer Metastasis Alert and Prevention Center, Fuzhou University, Sunlight Building, 6FL, Science Park, Xueyuan Road, University Town, Fuzhou 350116, China.
E-mail addresses: cmapcjia1234@163.com, jiali@fzu.edu.cn (L. Jia).

https://doi.org/10.1016/j.ebiom.2019.03.018

Research in context

Evidence before this study

Studies based on Suzanne LTopalian's review reported that blockade PD-1/B7-H1 (PD-L1) pathway could activate anti-tumor immunity especially adaptive immune. And based on Timo K.van den Berg' review, CD47 could regulate the innate immune. Besides, many articles on CD47 and PD-L1 regulation of immunity were reported separately.

Added value of this study

In our study we designed EpCAM (epithelial cell adhesion molecule)-targeted cationic liposome (LPP-P4-Ep) containing si-CD47 and si-PD-L1 could effectively target high-EpCAM cancer cells and knockdown both CD47 and PD-L1 proteins.

Implications of all the available evidence

Our results showed that we synthesized EpCAM-targeted cationic liposomes (LPP-P4-Ep) knockdown both CD47 and PD-L1 proteins which blocked CD47/SIPR-α and PD-L1/PD-1 axis. And dual-blockade CD47 and PD-L1 tumor cell-specific innate and adaptive checkpoints could effectively improve immunotherapy function.

as a negative checkpoint for innate immunity and subsequent adaptive immunity, which has emerged as one of the most promising new targets for immuno-oncology [16].

A number of recent studies have demonstrated the enhancement therapeutic efficacy of dual-blocking, anti-CD47 and anti-PD-L1, in the treatment of melanoma [17] and colon carcinoma [18]. However, in vivo antibody-based therapeutics by mechanically injection plays a biological functions on the same molecules that are expressed in the cytoplasmic membrane, regardless of their cellular population [19]. The defect limits antibody-based therapy application because some checkpoints such as CD47 are ubiquitously expressed on all cell populations, particularly hematopoietic cells. To avoid these undesired side effects, we used RNA interference (RNAi) therapy to inhibit PD-L1 and CD47 checkpoints on cancer cells. Meanwhile, liposomes may be the most successful and widely used in drugs and gene delivery systems among all non-viral carriers [20].

A recent study demonstrates the feasibility of oncogenic-driven co-expression of CD47 and PD-L1 for tumorigenesis [21]. In this research, we examined the CD47, PD-L1 and EpCAM expression levels in a series of tumor cell lines. Both CD47 and PD-L1 are highly expressed on tumor cells and serve as innate and adaptive checkpoints [18]. After confirmation of inhibitory effects by RNAi in cancer cells, we designed EpCAM-targeted cationic liposomes (LPP-P4-Ep) knockdown both CD47 and PD-L1 proteins which blocked CD47/SIPR-α and PD-L1/PD-1 axis. The hypothesis was tested in lung cancer cells PC-9 and mice cancer cells 4 T1. The pharmacodynamics of blocking CD47 and PD-L1 by RNAi therapy was evaluated in 4 T1 solid tumor models and lung metastatic models. Last but not least, the systemic toxicities in mice blood that received multiple doses of LPP-P4-Ep were examined.

2. Materials and methods

2.1. Materials

DOPE (Dioleoylphosphatidylethanolamine) was obtained from A.V.T (Shanghai) pharmaceutical Co, Ltd. DC-Chol (3β-[N-(N′, *N*′-Dimethylaminoethane) carbamoyl] cholesterol) was purchased from absin bioscience Inc.(Shanghai). MAL-PEG-COOH (Maleimide-(ethylene glycol)-carboxyl, average MW 3400 Da) was obtained from Shanghai Ponsure Bio, Inc. The high performance liquid Chromatography (HPLC)-purified anti-EpCAM DNA aptamer (Ep, sequence: HS-5′-CAC TAC AGA GGT TGC GTC TGT CCC ACG TTG TCA TGG GGG GTT GGC CTG-3′, 48 bp, MW = 15 k Da) with or without Cy5 modification was synthesized by sangon Biotech Co., Ltd.(Shanghai, China). All siRNAs were dissolved or diluted to a concentration of 20 μM in diethyl pyrocarbonate (DEPC) water (Invitrogen) and listed in Table 1.

Anti-mouse CD45-FITC, anti-mouse CD3e-PE, anti-mouse CD8a-PerCP-Cyanine5.5, anti-mouse CD49b (Integrin alpha 2)-PE-Cy7, mouse anti-human CD47-FITC, mouse anti-human PD-L1-APC, anti-mouse CD47-FITC, anti-mouse PD-L1-PE and anti-mouse EpCAM-PE were obtained from eBioscience. Mouse anti-human EpCAM-PE and CBA (Cytometric Bead Array) mouse Th1/Th2/Th17 cytokine kit were obtained from Becton Dickinson (BD) Pharmingen™. Carboxy fluorescein succinimidyl easter (CFSE), PKH26, PKH67, Hoechst 33258 and fluorescent dyes propidium iodide (PI) were purchased from Sigma-Aldrich. Rabbit anti-human CD47 antibody and rabbit anti-human PD-L1 antibody were obtained from Abcam. Human cytokine ELISA kit IL-6, human cytokine ELISA kit IFN-γ, mouse cytokine ELISA kit IL-6 and mouse cytokine ELISA kit IFN-γ were purchased from Lianke Biological Co., Ltd. All other unlisted materials are of analytical grade. Anti-mouse PD-L1 antibody was obtained from Wanlei Biotechnology, Inc. Anti-mouse CD47 antibody was obtained from Abcam. Anti-mouse β-actin antibody was purchased from Beijing Dingguo Biotechnology, Inc.

2.2. Synthesis of MAL-PEG-DOPE

Synthesis of MAL-PEG-DOPE refers to previously published articles [22,23]. The conjugation of carboxyl groups of MAL-PEG-COOH to the amine groups of DOPE was accomplished using the EDC/NHS technique. The process was carried out as follows: 30 mg carboxyl-modified PEG was dissolved in dichloromethane and mixed with EDC (5 mg) and NHS (4 mg). The solution was stirred continuously for 2 h at room temperature. Subsequently, 8 mg DOPE (MAL-PEG-COOH: DOPE =1:1, molar ratio) was added, and the reaction proceeded overnight under nitrogen. The reaction product was dried out most dichloromethane in rotary evaporator and then added to cold acetonitrile. The unreacted DOPE was centrifuged at 2414*g* for 10 min which was insoluble in cold acetonitrile. And the supernatant was dried to thin lipid in rotary evaporator. The film was hydrated with DD water. The reaction product was enclosed in dialysis bag (MW = 8 k Da) and transferred into 50 mL of DD water solution to separate free EDC/ NHS/ MAL-PEG-COOH at room temperature for 48 h. The final product DOPE-PEG-MAL was subsequently freezed by lyophilizer. To confirm the DOPE-PEG-MAL conjugation, the samples were examined by nuclear magnetic resonance spectroscopy.

Table 1
CD47, PD-L1 and EpCAM expression in surface abundance of tumor cells.

	Cells	CD47	PD-L1	EpCAM
Lung cancer cells	PC-9	99.5%	84.3%	99.5%
	A549	99.9%	99.3%	10.6%
	H1975	99.7%	99.9%	79.0%
	Helf	2.57%	3.83%	1.18%
	H1299	99.7%	63.5%	14.0%
	SPAC-1	94.8%	60.5%	99.8%
Breast cancer	MCF-7	99.6%	9.47%	81.6%
	MDA-MB-231	38.2%	9.37%	99.3%
	MDA-MB-435	98.5%	14.5%	99.8%
Mice cancer cells	4 T1	99.7%	78.2%	98.8%
	B16F10	99.7%	92.4%	43.7%
	LLC	99.3%	74.8%	12%
	CT26	99.8%	91.9%	21.6%

Note: positive rate <10% is not expressed; 10%≤ positive rate ≤30% for low expression; 30% < positive rate ≤ 60% for medium expression positive rate >60% for high expression.

2.3. Preparation of black liposomes

The steps for the synthesis of liposomes were based on published articles [24]. and with minor modifications [25,26]. Briefly, MAL-PEG-DOPE, DOPE and DC-Chol at a molar ratio of 0.1: 1:1(about 8 μmol total lipids) ware dissolution in 10 mL dichloromethane and then the lysate were dried into thin lipid film in a rotary evaporator. The film was hydrated using DD water (**LPP**). After that, si-CD47 or/and si-PD-L1 and LPP complexes were gently mixed to form **LPP-4 /LPP-P /LPP-P4** complexes. The **LPP-4 /LPP-P /LPP-P4** complexs were formed by electrostatic interaction between positive (liposomes) and negative charges (siRNA). DC-Chol and DOPE were used to prepare liposome complexes (**LP**) with the similar process, except the MAL-PEG-DOPE was not added. All liposomes are stored at 4 °C before use.

EpCAM was combined with LPP using the method published by Wu [27]. Eight micromoles of liposomes with MAL-activated PEG-DOPE on the surface were incubated with HS-EpCAM at a ratio of 10:1 for 24 h at 4 °C in darkness. Ultrafiltration was used to remove small molecular weight residues in LPP-Ep solution (50 k MWCO, Millipore, USA), and then the solution was resuspended in DD water. Cy5 modified LPP-Ep **(LPP-Ep-Cy5)** was prepared with the same process.

The uniform naming of synthetic materials: **LPP-P4-Ep** for liposome-PEG-EpCAM contained si-PD-L1 and si-CD47, **LPP-P-Ep** for liposome-PEG-EpCAM contained si-PD-L1, **LPP-4-Ep** for liposome-PEG-EpCAM contained si-CD47, **LPP-Ep** for liposome-PEG-EpCAM, **LPP** for liposome-PEG without aptamer, **LP** for liposome without any aptamer or PEG.

2.4. Characterization of LPP-Ep liposome

To confirm EpCAM conjugation, LPP-Ep or EpCAM free was analyzed by agarose electrophoresis refer to *Cheng*[20]. Samples loaded were as follows: 1, LPP-Ep; 2, EpCAM; 3, LPP; 4, mixture of EpCAM and LPP; 5, 10 bp marker. The electrophoresis was managed for 30 min at 80 V, and then the gel was stained with Syber Gold for 30 min at room temperature in the darkness.

To calculate EpCAM conjugation amount, the standard solutions of Ep-cy5 were analyzed by fluorescence spectrophotometer (F-7000, Hitachi, Varian Ltd., USA). The binding efficiency of EpCAM-Cy5 with liposomes was detected by collecting the unbounded EpCAM-Cy5 after ultrafiltration and calculating their conjugation concentration. Binding concentration of both was presented as mean ± SEM and calculated from the standard curve of Cy5 fluorescence intensity. Binding concentration = adding total concentration - unbounded concentration under ultrafiltration. (Cy5 under $\lambda_{ex} = 647$ nm and $\lambda_{em} = 670$ nm).

To evaluate the characteristics of the liposomal formulations, the mean particle size and zeta potential of a series of liposome complexes were measured using a Malvern Instruments Zetasizer HS III (Malvern UK) at room temperature. Each batch was analyzed in triplicate. Scanning electron microscope (SEM), transmission electron microscopy (TEM) and atomic force microscopy (AFM) system (Bruker, USA) were used to detect the morphology of **LPP-Ep**.

Agarose gel electrophoresis was used to detect si-CD47 or si-PD-L1 loading ability of LPP-Ep. The 50 nmol si-CD47 or si-PD-L1/liposome complexes were added to agarose gel in TAE buffer. The N/P ratio of **LPP-Ep/siRNA** was 1, 2, 3, 5, 10, 20, 30. The electrophoresis was managed at 80 V for 30 min, and then the gel was stained with Syber Gold for 30 min at room temperature in the darkness.

To test the stability of siRNA, LPP-Ep containing siRNA was co-incubation with 1640, PBS and FBS. After different time, LPP-Ep was lysis using 2% heparin sodium. The stability ability of siRNA was tested by agarose gel.

In vitro si-CD47-FAM and si-PD-L1-Cy5 release experiments with LPP-P4 and LPP-P4-Ep were performed in 1 mL PBS solution with 5.6 and 7.4 pH values (FAM under $\lambda_{ex} = 493$ nm and $\lambda_{em} = 520$ nm; Cy5 under $\lambda_{ex} = 647$ nm and $\lambda_{em} = 670$ nm). The method was as following: 1 mL of LPP-P4 or LPP-P4-Ep solution was placed in a dialysis bag (MW = 50 k Da) and then immersed in 5.6 or 7.4 PBS solution. The process reaction was kept at 37 °C., 200 uL of each sample was collected at different time points and the total siRNA released from LPP/LPP-Ep complexes was detected using fluorescence spectrophotometer at 493 nm and 647 nm and calculated the concentration through the standard curve. The release result was repeated three times and the results were expressed as mean ± SEM.

2.5. In vitro cell assays

The HELF, A549, PC-9, H1975, H1299, SPCA-1, MCF-7, MDA-MB-231, MDA-MB-435, 4 T1, B16F10, LLC, and CT26 cells were purchased from the Cell Resource Center of Shanghai Institute for Biological Sciences (Chinese Academy of Sciences, Shanghai, China). The PC-9, H1299, SPCA-1, MCF-7, 4 T1, B16F10, LLC, CT26 and A549 cells were cultured in 1640 RPMI medium containing 10% FBS and 1% penicillin-streptomycin (*v*/v). The HELF, MDA-MB-231, MDA-MB-435 and H1975 cells were grown in DMEM medium supplemented with 10% FBS and 1% penicillin-streptomycin (v/v). The cells were maintained in a humidified cell incubator at 37 °C with 5% CO_2.

HELF, A549, PC-9, H1975, H1299, SPCA-1, MCF-7, MDA-MB-231 and MDA-MB-435 cells were respectively stained with mouse anti-human CD47 (FITC-labelled), mouse anti-human PD-L1 (CD274) (APC-labelled) and mouse anti-human CD326 (EpCAM) (PE-labelled) antibody and incubated at 4 °C for 30 min in the dark. B16F10, 4 T1, LLC, and CT26 cells were respectively stained with anti-mouse CD47 (FITC-labelled), anti-mouse PD-L1 (PE-labelled) and anti-mouse EpCAM (PE-labelled) antibody and incubated at 4 °C for 30 min in the dark. Background staining was performed by staining cells with isotype-matched control. After staining, cells were washed with the staining buffer (2% FBS, 2 mM EDTA in PBS) and resuspended in 500 μL of the staining buffer. Flow cytometric analysis was carried out on the BD FACSAriaIII (BD Biosciences), and the obtained data were analyzed with FlowJo software.

To analysis the apt-EpCAM-mediated targeting, confocal cytometry and flow cytometry were used to detect a binding specificity assay on A549, PC-9 and HELF cells. EpCAM-negative cells Helf were used as control. Helf, PC-9 and A549 cells were seeded in 6-well plates with 10% FBS medium in flow cytometry analysis. After 24 h, cells were incubated with 1640 medium containing 1, 10, 25, 50, 100 nM Cy5-EpCAM for 4 h or fresh medium containing 50 nM Cy5- EpCAM for 1, 2, 4, 6, 8 h. After washing with PBS, cells were digested and then detected by flow cytometry.

For quantitative comparison of siRNA uptake efficiency, FAM-siCD47 and Cy5-siPD-L1 mean on PC-9, A549, HELF and 4 T1 cells were measured by confocal imaging and flow cytometry. Briefly, 5×10^4 cells were seeded into 6 well plates and incubated for 24 h. Each cells were incubated medium with LPP-Ep containing FAM-siCD47 and Cy5-siPD-L1 (the dose of each siRNA was 50 nmol) for another 4 h. After that, cells were washed three times with PBS. Confocal microscope was conducted to get fluorescence imaging with different wavelengths to determine FAM-siCD47 and Cy5-siPD-L1 intake effect. Green and red fluorescence means were evaluated by BD FACSAria III. Background comparison was performed by same concentration FAM-siCD47 and Cy5-siPD-L1 alone.

To prove the silencing efficiency of CD47 and PD-L1 proteins in PC-9 and 4 T1, the cells were transfected with different formulation, including LPP-NC-Ep, LPP-4-Ep, LPP-P-Ep and LPP-P4-Ep with FBS free medium at different dose of siRNA for 6–8 h. And then cells were harvested with normal medium for another 48 h or 72 h and washed three times with PBS. Detection step refers to step 2.5.2.

The inhibition of EpCAM was also detected by flow cytometry. Detection step refers to step 2.5.2. PC-9 cells were also incubation with free aptamer EpCAM at different concentrations for 24 h, the expression of EpCAM was detected by flow cytometry.

Cytotoxicity of LP, LPP, LPP-Ep was assayed by MTT assay in HELF, A549, PC-9 and 4 T1 cell lines. The 10,000 cells were seeded into 96-well plates for per well. After 24 h, medium with LP, LPP, LPP-Ep complexes at 50 nM concentration siRNA was added. After continued incubation for 48 h, the cytotoxicity effect for different complexes was assessed by the MTT assay. Meanwhile, PC-9 cells were incubated with LPP-Ep, LPP-4-Ep, LPP-P-Ep and LPP-P4-Ep complexes at a dose of 50 nM siRNA concentration without changing culture medium. The absorbance at 490 nm was determined by a microplate reader. Normal cultured cells served as control group. All samples were repeated 5 times.

A flow cytometric, target-based cytotoxicity assay was conducted according to methods previously published [28,29]. Peripheral blood mononuclear cells (PBMCs) from anonymous healthy donors were obtained from Fujian Provincial People's Hospital Affiliated to Fujian University of Traditional Chinese Medicine (Fuzhou, China). Monocytes were isolated from Ficoll-Isopaque density centrifugation. The samples were stored at 4 °C and processed within 6 h after their collection. Target cells PC-9 were labelled with 3 μM CFSE (from a 1 mM stock solution in dimethyl sulfoxide) in phosphate-buffered saline (PBS) for 15 min at 37 °C in a volume of 1 mL and then washed twice with PBS. Labelled cells were immediately seeded in 6-well culture plates at a density of 5×10^4 cells/well for 24 h. After transfected by FBS free medium with LPP-Ep, LPP-NC-Ep, LPP-4-Ep, LPP-P-Ep and LPP-P4-Ep liposomes complexes (50 nM), the CFSE labelled-PC-9 were mixed with effect cells monocytes at T: E ratios 1:10. In parallel, PC-9 cells incubated monocytes alone was measure as basal apoptosis. Cells were incubated for 36 h at 37 °C in a humidified atmosphere of 5% CO_2 and then harvested with 0.25% trypsin (GenView). Cells were washed in PBS-1% FBS and incubated with 500 uL of PI (1 μg/mL) for 15 min at 37 °C in the dark before determined. CFSE-labelled cells can distinguish the target cells and effect cells. While PI (Propidium iodide) was added to determine the ratio of cell death. Flow cytometric analysis data were collected on the BD FACSAria III, and the obtained data were analyzed with FlowJo software.

For cytokines detection, 10^5 cancer cells were plated in 6-well round-bottom microplates for per well and incubated overnight. Cells were treated by LPP-Ep, LPP-NC-Ep, LPP-4-Ep, LPP-P-Ep and LPP-P4-Ep liposome complexes. The original medium was removed, and fresh medium or medium containing monocytes was added to the wells at an E/T of 10:1. The cancer cells and monocytes were incubated in an incubator for 24 h. ELISA was performed on the supernatants using a human cytokine ELISA kit (Lianke) to quantify IFN-γ and IL-6 secretion.

2.6. Tumor growth inhibition in vivo

Cells 4 T1 were harvested and suspended in PBS with concentration 5×10^5 cells/100 uL. Balb/C mice were inoculated with 4 T1 cells by subcutaneously injecting 5×10^5 4 T1 cells in 100 uL PBS on the hind legs. When the tumor volumes reached 100 mm^3, Balb/C mice were treated by LPP-P4-Ep complexes from 14th day after inoculation. LPP-Eps containing 8 μg CD47 or/and PD-L1 or control siRNA (about 0.4 mg/kg) were subcutaneously injected every two day for a totally of 5 treatment. Digital caliper was used to calculate tumor size. The tumor volume formula was (1/2 × length ×width [2]).

To detect biodistribution of LPP-Ep in 4 T1 model mice, Balb/C mice were injected with PBS (control) containing LPP linking Cy5-EpCAM (0.4 mg/kg) via subcutaneous injection. After 2, 4 and 12 h, mice were executed. The tissue samples (tumor, heart, liver, spleen, lung and kidney) were collected. Similarly, part of tissue samples were prepared by a freezing microtome in 7 um. Nucleus were stained with Hoechst 33258 and florescence intensity of Cy5 was observed by confocal microscope.

The tissues including heart, liver, spleen, lung, kidney and tumor were executed. And then they were dehydrated, embedded in paraffin, and stained with hematoxylin and eosin (H&E). Histological observations were examined by a microscope (Zeiss, Germany). Before soaking with formaldehyde, the weight of the spleen s is weighed with an electronic balance. Spleen size was measured with digital caliper. After the sacrifice of the mice, six groups of tumors mRNA and proteins were collected. The method of RT-PCR referred to *Cheng* [30] to detect mRNA and the method of western blot referred to *Lian* [31] before to detect CD47, PD-L1 and β-actin proteins.

Immunofluorescence assay of CD47 and PD-L1 in tumor tissues was executed using paraffin sections. Tissues were sliced into 4.5 μm and blocked by 5% BSA for 2 h, and then incubated with anti-CD47/anti-PD-L1 antibodies (Abcam) overnight at 4 °C. After that, the slides were incubated with FITC-labelled goat anti-rabbit secondary antibody, and then washed with PBS and stained with Hoechest 33258.

Mice blood samples were collected from the mice eyes with the capillaries. Fifty microliter of mice blood was drawn from each mice and collected in 1.5 mL EP tube containing ethylenediaminetetraacetic acid. Cells were incubated with anti-mouse CD19a, anti-mouse CD3, anti- mouse CD45, anti- mouse CD8a and anti- mouse CD49b for 30 min at 4 °C in the dark. Ten-fold volume of red blood cell lysis buffer was then added to the blood to remove the red blood cells (RBCs). Cell suspensions were pooled and centrifuged 300 *g* for 5 min at room temperature. Cells were washed with PBS-1% FBS for twice before determined. Flow cytometric analysis data were collected on the BD FACSAria III (BD Biosciences), and the obtained data were analyzed with FlowJo software.

After the final administration for 2 days mice were executed and tumors were separated for ELISA analysis. The tumor was lysed and the solution was collected. ELISA was performed on the solution using a mouse cytokine ELISA kit (Lianke) to quantify IFN-γ and IL-6 secretion. The cytokines of the blood were determined by collecting supernatant before the mice were sacrificed. Mice blood samples were collected from the mice eyes with the capillaries. All samples, kit controls and standards were analyzed in triplicate.

2.7. Metastasis inhibition assay invivo

PBS containing 1×10^5 4 T1 cells/100 μL was injected to Balb/C via tail vein to build metastasis model. LPP-Ep containing 8 μg si-NC or si-CD47 or/and si-PD-L1 (0.4 mg/kg for each) were injected to each mice through tail. Injection begins on the 14th day of inoculation and is given every 3 days. Mice were sacrificed and tissues were harvested on day 39 after inoculation.

The tissue distribution in metastasis model measurement method was consistent with subcutaneous tumor model refering to Method **2.6**.

The mice blood was collected from 10 days after injection different LPP-Ep complexes. And immune cells collection method is consistent with Method 2.6. CBA assay was executed to detect the cytokines of IL-10, IL-17A, TNF, IFN-γ, IL-6, IL-4 and IL-2. The procedure was described as followed: mice blood samples were collected from the mice eyes with the capillaries. Fifty microliter of mice blood was drawn from each mice and collected in 1.5 mL EP tube containing ethylenediaminetetraacetic acid. The supernatant was centrifuged through 300 *g* for 10 min. Detection steps refer to CBA instructions.

Histopathology analysis method refers to method **2.6**. After treatment, whole blood collected from the mice were assayed for hematology parameters. Tissues including heart, liver, spleen, lung and kidney were collected for hematoxylin and eosin assay.

2.8. Ethics statement

All animal experiments were approved by the Institutional Animal Care and Use Committee of Fuzhou University and operated following the NSFC regulations concerning the care and use of experimental animals. Balb/C female mice (about 20 g weight, 4–6 weeks old) were obtained from Fuzhou Wushi Animal Center. The healthy human blood collection procedure was carried out in accordance with the guidelines

verified and approved by Fujian Provincial People's Hospital Affiliated. All donors signed an informed consent for scientific research statement.

2.9. Statistical analysis

Graphpad Prism 5.0 (Graphpad software, San Diego, CA) was used for all statistical analysis. The mean ± S.E.M. was determined for each treatment group in the individual experiments, and the standard *t*-test was used to determine the significances between treatment and control group(s). *P*-values <0.05 were significant. Statistical analyses were performed with the SPSS statistical software package.

3. Results

3.1. Synthesis of LP, LPP and LPP-Ep

Firstly, DC-Chol, DOPE and MAL-PEG-DOPE were prepared for liposome LPP and then aptamer EpCAM that specifically targets high-EpCAM tumor cells were conjugated onto the surface of liposomes. The synthetic procedures for LP, LPP and LPP-Ep are showed in Fig. 1. Firstly, DOPE was connected to MAL-PEG-COOH by carboxyl and amino reactions. The primary amine groups of DOPE were covalently conjugated to carboxyl of MAL-PEG-COOH by EDC/NHS catalysis to generate the MAL-PEG-DOPE conjugate. The conjugation synthesis of MAL-PEG-DOPE was confirmed by Nuclear Magnatic Resonance (NMR), which was showed in Fig. S1. The characteristic peaks of DOPE showed the succeed synthesis of DOPE-PEG- MAL.

After successful synthesis of MAL-PEG-DOPE, HS-EpCAM with thiol group was designed to react with MAL-PEG-DOPE containing maleimide groups at buffer solution. To confirm the conjugation of aptamer HS-EpCAM to LPP, agarose electrophoresis was run (Fig. 2a). Since aptamer EpCAM showed negative charges, LPP displayed positive charges. Aptamer EpCAM alone showed a band at the small molecular weight (Fig. 2a, line 2). When aptamer EpCAM was covalently conjugated with LPP, a smeared band at the opposite loading site appeared (Fig. 2a, line 1). LPP itself did not show any band (Fig. 2a, line 3). The immediate mixture of aptamer EpCAM and LPP showed band with the same band result of LPP-Ep (Fig. 2a, line 4), indicating that the reaction was very fast. These data indicated that aptamer EpCAM could strongly and rapidly connect with the surface of LPP. Besides, the connection amount between LPP and EpCAM was also determined by fluorescence spectrometer which was about 200 uM/mL (Fig. 2b).

The synthesis steps of LPP-Ep were shown in the Method [24]. A range size and potential of liposome complexes were analyzed by DLS. All liposomes have a particle size of about 120–175 nm and a uniform particle size and positive zeta potential (Fig. 2 and Table S2). The diameters and the size distributions of LPP-Ep, LPP-P-Ep/LPP-4-Ep and LPP-P4-Ep measured by DLS showed only a slight increase after single or dual siRNA loading. The results of LPP-P4-Ep observed from TEM, SEM and AFM was also about 175 nm, which consisted to DLS data (Fig. 2c-e). The zeta potential of LPP-P4-Ep decreased to 31.7 mV showed that the biological toxicity would be reduced due to the decrease of strong positive charges [32] (Table S2).

To evaluate the dual siRNA release behavior from LPP and LPP-Ep, and LPP and LPP-Ep were incubated in pH 5.6 and 7.4, respectively, and the released FAM-si-CD47 and Cy5-si-PD-L1 were analyzed at the setting time (Fig. 2g). In pH 5.6 and 7.4 conditions, the release rates of total siRNA from LPP and LPP-Ep were relatively slow and then reached a stable state after 8 h. The release percentage of total siRNA in pH 7.4 only was 10%, which was half of release percentage in pH 5.6. The standard curve lines of FAM-siCD47 and Cy5-siPD-L1 were listed in Fig. S3.

The optimal N/P ratio about siRNA and LPP-Ep is also discussed by a gel retardation assay. The N/P ratios from 1:1 to 5:1 appeared obviously bands which was agreed with the single nucleic acid bands, however, the band disappeared when the N/P ratio was up to 10:1 (Fig. S2). These results provided an optional and suitable N/P ratio between siRNA and LPP-Ep in vitro and in vivo for future biological experiments. LPP-Ep containing siRNA in 1640 medium, PBS and FBS for 24 h still maintained high concentration (Fig. S3). LPP-Ep could keep siRNA stable.

3.2. High expression of three proteins and effective cellular uptake

The expression levels of CD47, PD-L1 and EpCAM were confirmed by Flow cytometry. As show in Table 1, the expression of CD47 and PD-L1 on lung cancer cells was generally higher than that of breast cancer cells. The expression percentage of EpCAM in PC-9 cells was about 99.9%, the expression percentage of EpCAM in HELF cells was about 1.18%, and the expression percentage of EpCAM in A549 cells was about 10.6%. Based on the results, PC-9 cells were selected as experimental positive cells, and HELF cells were chosen as negative cells for experiments.

Flow cytometry was used to detect the binding ability of the aptamer EpCAM to recognize EPCAM over-expressed PC-9 cells. In Fig. 3a-b, after incubation with Cy5-EpCAM aptamer, PC-9 fluorescence mean intensity was significantly higher than that of control. Meanwhile, low Cy5 fluorescence intensities were measured in the EpCAM-negative HELF and A549 cells.

LPP-P4-Ep cell uptake on PC-9, A549 and Helf cells was detected by confocal laser scanning microscopy and flow cytometry. LPP and LPP-Ep loaded with FAM-siCD47 and Cy5-siPD-L1 were incubated with EpCAM-positive PC-9 cells, EpCAM-low A549 and EpCAM-negative HELF cells at 37 °C for 4 h. After transfection with fluorescent labelled LPP-P4-EP, PC-9 cells showed strong green and red fluorescence, low fluorescence on A549 cells and almost no fluorescence on HELF cells. (Fig. 3). Therefore, in the following experiments, PC-9 cells were selected as target cells, because they were highly expressed in CD47 and PD-L1 and could be effectively recognized by aptamer EpCAM.

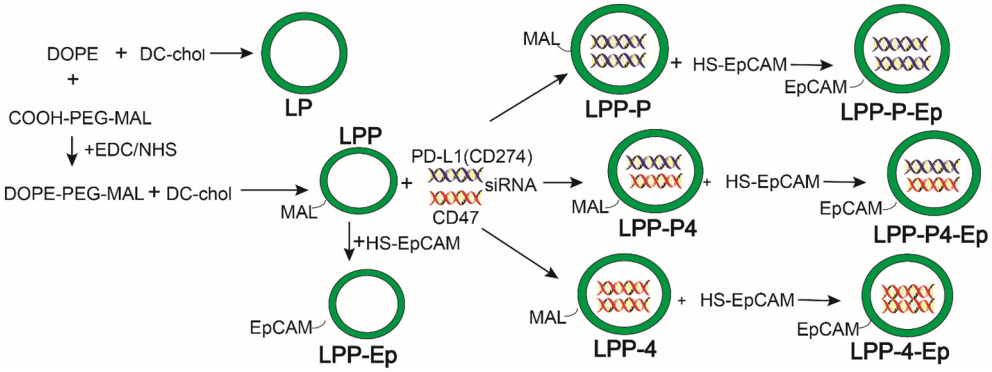

Fig. 1. Schematic illustration of the design and synthesis of LP, LPP, LPP-Ep, LPP-P, LPP-4, LPP-P4, LPP-P-Ep, LPP-4-Ep and LPP-P4-Ep complexes.

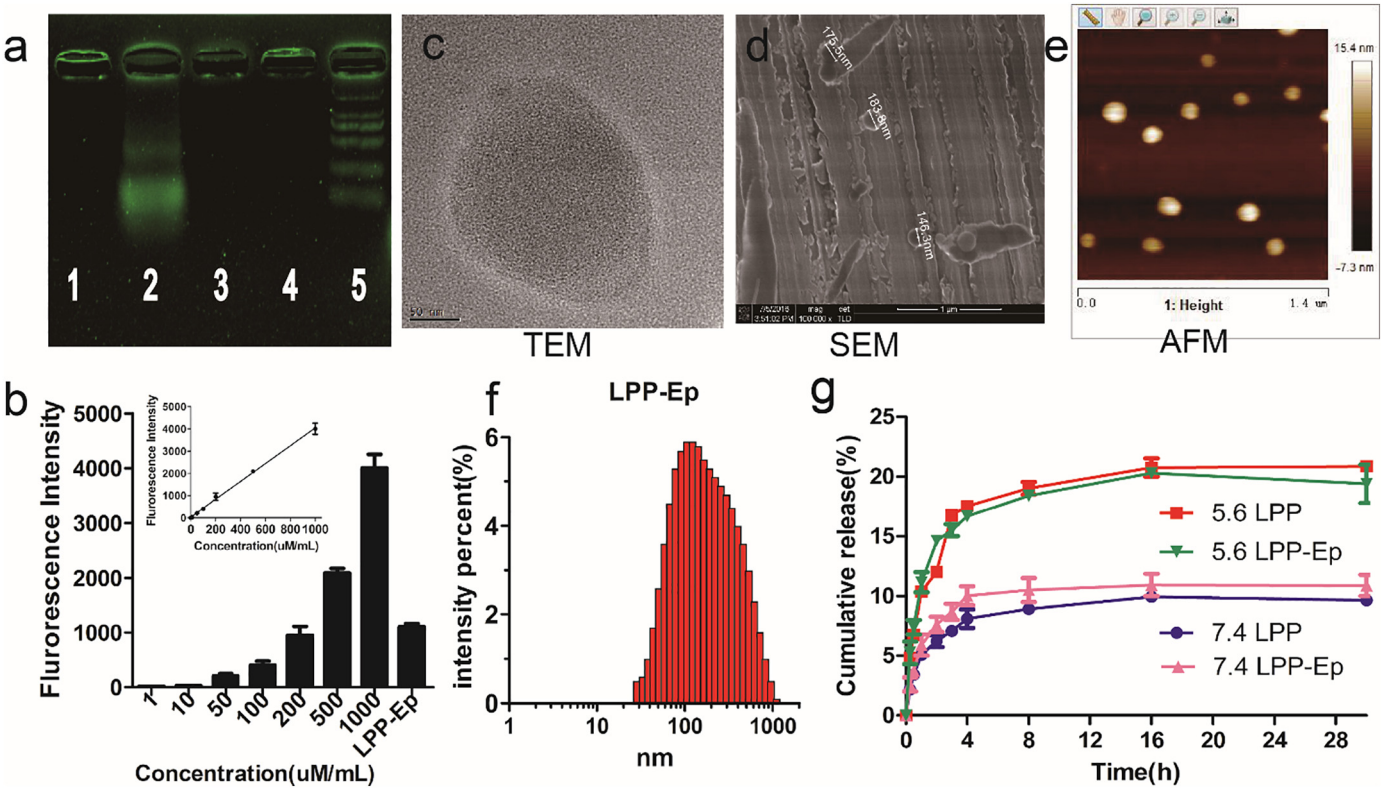

Fig. 2. Characteristics of LPP-Ep. (a) Identification of aptamer EpCAM binding to LPP. (1, LPP-Ep; 2, EpCAM; 3, LPP; 4, mixture of EpCAM and LP-P; 5, marker). (b) The relationship between fluorescence intensities and quality control concentrations of Cy5-labelled LPP-Ep. (c-e) TEM, SEM and AFM images of LPP-Ep liposome; (f) Hydrodynamic diameter of LPP-Ep; (g) The release of siRNA from LPP and LPP -Ep in 5.6 or 7.4 pH PBS solution in vitro. The results were repeated three times and the error bars expressed as mean ± SEM.

3.3. LPP-P4-Ep cytotoxicity assays, cells gene silencing and co-incubation toxicity

It is commonly believed the relation to an electrostatic interaction between the positive charge of cationic liposomes and the negatively charged glycocalyx of endothelial cells. In-vitro cytotoxicity of blank cationic liposomes and liposomes encapsulated CD47 and PD-L1 siRNA was determined using the MTT assay [33]. After incubation with LP, LPP and LPP-Ep complexes for 24 h, the survival rate of 4 T1 cancer cells and normal cells HELF maintained nearly 100%, but there were slightly toxic to PC-9 cells. (Fig. 4a). However, after being incubation with LPP-Ep contained CD47 and PD-L1 dual siRNA, the cells viability maintained nearly 95% for PC-9 cells (Fig. 4b). These results indicated that LPP-P4-Ep complexes were less cytotoxic to PC-9 cells, 4 T1 cells and HELF cells.

The inhibition ability of LPP-P4-Ep in functional CD47 and PD-L1 siRNA was confirmed by dual protein expressions in PC-9 cells (Fig. 4c-h). Both LPP and LPP-Ep contained target siRNA can effectively interfere with the proteins expression of CD47 and PD-L1, and the LPP-Ep group has obvious interference effects than LPP group (Fig. 4c-d). Compared to negative control, CD47 protein expression decreased at 48 h and reduced significantly till 72 h after transfection with LPP-4-Ep (si-CD47 at s dose of 25 nM). In addition, there was no significant change in the expression level of CD47 protein treated with LPP-NC-Ep or si-CD47 alone. The inhibitory result of PD-L1 protein is the same as that of CD47 (Fig. 4g-h). These results implied that LPP-P4-Ep can effectively inhibition of CD47 and PD-L1 proteins expression through RNAi regulation. Besides, the expression of EpCAM on PC-9 cells was detected by flow cytometry which was inhibited by aptamer EpCAM and decreased gradually with the increase concentration of EpCAM (Fig. 4i).

After confirming the interference effect of LPP-P4-Ep, monocytes were isolated from peripheral blood mononuclear cells. PC-9 cells were stained with CFSE, and transfected by different liposome complexes. Monocytes were added to the PC-9 cells at a ratio of 10:1. After 36 h all cells were collected and stained with PI. Data were collected regarding CFSE-positive, PI-positive, and double-positive events (Fig. 4j), the last events interpreted as immune effect between monocyte effectors and tumor cell targets and shown in the column diagram (Fig. 4k). PC-9 cells transfected by either CD47 or PD-L1 groups showed strongly toxicity compared to the control group. It is exciting that double RNA interference cells showed lower survival rate compared with single RNA interference. These results indicated that CD47 coordination with PD-L1 may have more effective immunotherapy effect.

After incubation with monocytes for 24 h, cell culture supernatants at an E/T of 10:1 were collected and analyzed for cytokine secretion using a specific ELISA kit. Synergetic inhibition of si-CD47 and si-PD-L1 increased cytokines such as IL-6 (9.6 ± 0.5% vs 5.6 ± 0.1%, $P < 0.01$) and IFN-γ (3.9 ± 0.9% vs 1.0 ± 0.2%, $P < 0.01$) compared to the control group (Fig. S5). These results indicated that blocking CD47/SIPR-α and PD-L1/PD-1 axis on cancer cells induced high cytokines secretion by monocytes to enable adjust immune response.

3.4. Systemic delivery of CD47 and PD-L1 siRNA in LPP-NPs inhibited solid tumor model

After confirming that CD47 and PD-L1 silencing could induce immune activation in vitro, we next evaluated the effect of systemic delivery of CD47/PD-L1 siRNA in Balb/c mice. First, in vitro target function and inhibition CD47 and PD-L1 proteins efficient of LPP-P4-Ep on 4 T1 were also determined in the same methods as PC-9 cells (Fig. S6). The results indicated that CD47 and PD-L1 proteins could effectively inhibited by LPP-P4-Ep.

In left leg of Balb/c mice were injected with 5×10^5 4 T1 cells. The mice received subcutaneous injections of LPP-P4-Ep every two days for a total of six injections. As was reported by *Chono* et al. [34], LPP-NPs loaded siRNA was minimally immune-stimulatory over a broad

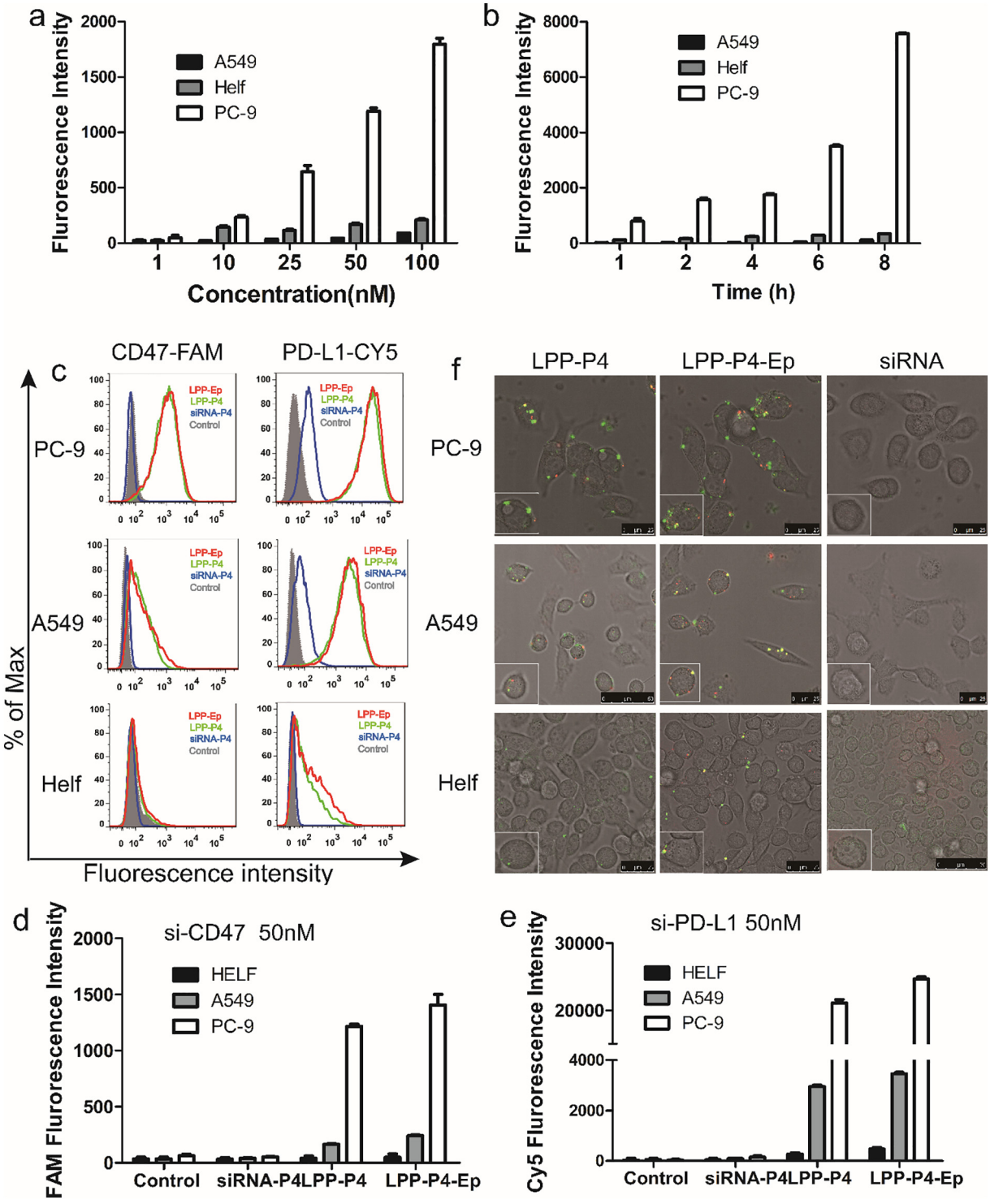

Fig. 3. Cell recognition ability of anti-EpCAM aptamer and cellular efficiency of EpCAM-targeted liposome complexes to PC-9, A549 and Helf cells. (a) The target capacity of Cy5-EpCAM on PC-9, A549 and Helf cells at concentration of 1, 10, 25, 50, 100 nM at 4 h. The error bars expressed as mean ± SEM (n = 3). (b) The target capacity of Cy5-EpCAM on PC-9, A549 and Helf cells at of 50 nM concentration at 1, 2, 4, 6, 8 h. The error bars expressed as mean ± SEM ($n = 3$). (c-e) Flow cytometry analysis of FAM-siCD47 and Cy5-siPD-L1 fluorescence intensity. PC-9, A549 and Helf cells treated with siRNA-P4, LPP-P4 and LPP-P4-Ep at 4 h. The data present means ± SEM (n = 3). (f) Cells were transfected with siRNA-P4, LPP-P4 and LPP-P4-Ep for 4 h. FAM-siCD47 (green) or Cy5-siPD-L1 (red) was imaged by confocal laser scanning microscope.

range of dose (0.15–1.2 mg/kg). As shown in Fig. 5a, there was no significant difference in body weight between the six groups, indicating the biocompatibility and safety of LPP-Ep complex in vivo. In terms of tumor growth, the delivery of CD47 and PD-L1 siRNA in an LPP-P4-Ep formulation can effectively inhibit solid tumor growth. After treatment, the volume of tumors decreased by 87% ($P<0.001$) compared with the untreated group. And the tumor volume treated by dual siRNA was reduced by 49% and 52% respectively compared with the use of siRNA CD47 or siRNA PD-L1 alone (Fig. 5b and d). Anti-CD47/PD-L1 antibody immunofluorescence assay was used to detect CD47/PD-L1 protein knockout level in tumor tissues. Fluorescence images, mRNA data and western blot results (Fig. 5c and Fig. S7) showed that CD47 and PD-L1

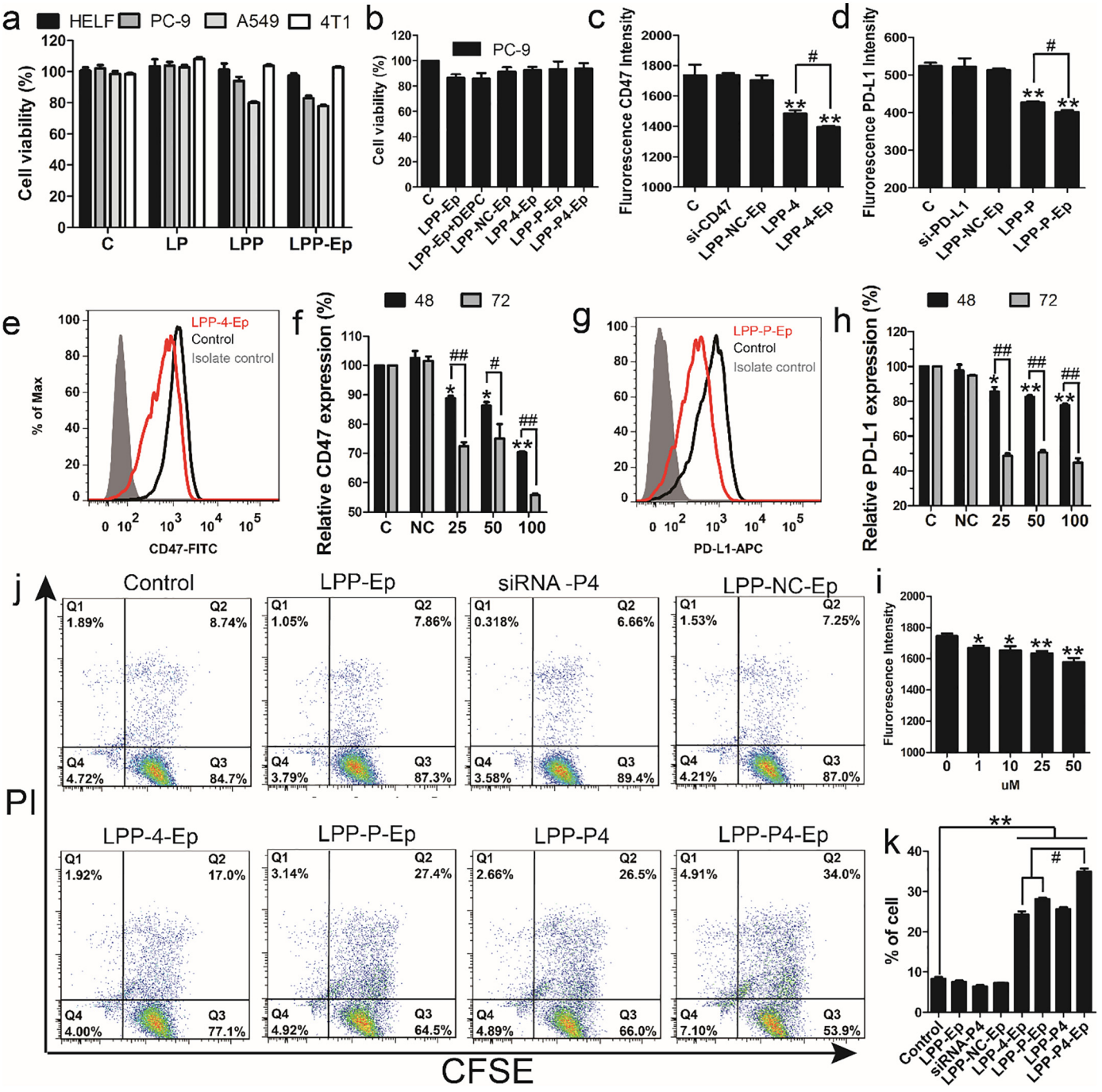

Fig. 4. The efficient function of LPP-P4-Ep. (a) Cell cytotoxicity of various formulations nanoparticles (LP, LPP and LPP-Ep) on HELF, PC-9, A549 and 4 T1 cells. (b) Cell cytotoxicity of various formulations of nanoparticles (LPP-Ep, LPP-NC-Ep, LPP-4-Ep, LPP-P-Ep and LPP-P4-Ep) on PC-9 cells. The cell viability was expressed as the percentage of the controls. (c-d) Down regulation of CD47 and PD-L1 protein expressions by LPP-4-EP/LPP-P-EP. (e-h) Down regulation of CD47 and PD-L1 protein expressions by LPP-P4-EP at 25, 50 and 100 nM siRNA concentration. $^{*}P < 0.05$, $^{**}P < 0.01$, $^{***}P < 0.001$ compared to the control group by ANOVA test. $^{\#}P < 0.05$, $^{\#\#}P < 0.01$ compared with the 48 h group by ANOVA test. (Ḥi) Down regulation of EpCAM protein expression by EpCAM aptamer. $^{*}P < 0.05$, $^{**}P < 0.01$, $^{***}P < 0.001$ compared with the control group by ANOVA test. (j) Monocyte cells were co-cultured with CFSE labelled PC-9 cells at ratio (E: $T = 10$: 1). (k) Column diagrams show $CFSE^{+}/PI^{+}$ (**Q2**) labeling cells percentage of (J). $^{*}P < 0.05$, $^{**}P < 0.01$, $^{***}P < 0.001$ compared with the control group by ANOVA test. $^{\#}P < 0.05$, $^{\#\#}P < 0.01$ compared with the LPP-P4-Ep group by ANOVA test. All error bars expressed as mean ± SEM.

were effectively silenced after LPP-P4-Ep treatment. Besides, spleen weight decreased slightly in each group, but there were no significant difference (Fig. 5e-f).

The distributions of LPP-Ep-Cy5 on heart, liver, spleen, lung, kidney and tumor were determined by confocal microscope at 2, 4 and 12 h. As shown in Fig. 6a, LPP-Ep showed relatively lower distribution in heart and kidney during 12 h. And LPP-Ep showed relatively high distribution in liver and lung in 2 h, and then reduced rapidly after 4 h. The accumulation of LPP-Ep in the spleen and tumor was significantly lower at 4 h but enriched at 12 h. These results demonstrated that LPP-Ep containing siRNA could be effectively delivered to tumor.

The IFN-γ and IL-6 cytokines in tumors and blood were determined by ELISA. We found that the dual siRNA treatment LPP-P4-Ep group mice contained significantly higher levels of both IFN-γ and IL-6 than those of the PBS control mice or single siRNA treatment mice (Fig. 6e-f). As shown in Fig. S8. a-b, the percentage of NK cells slightly increased in LPP-P4-Ep group compared to other group. These results indicated that immunization with dual checkpoints inhibition induced immune

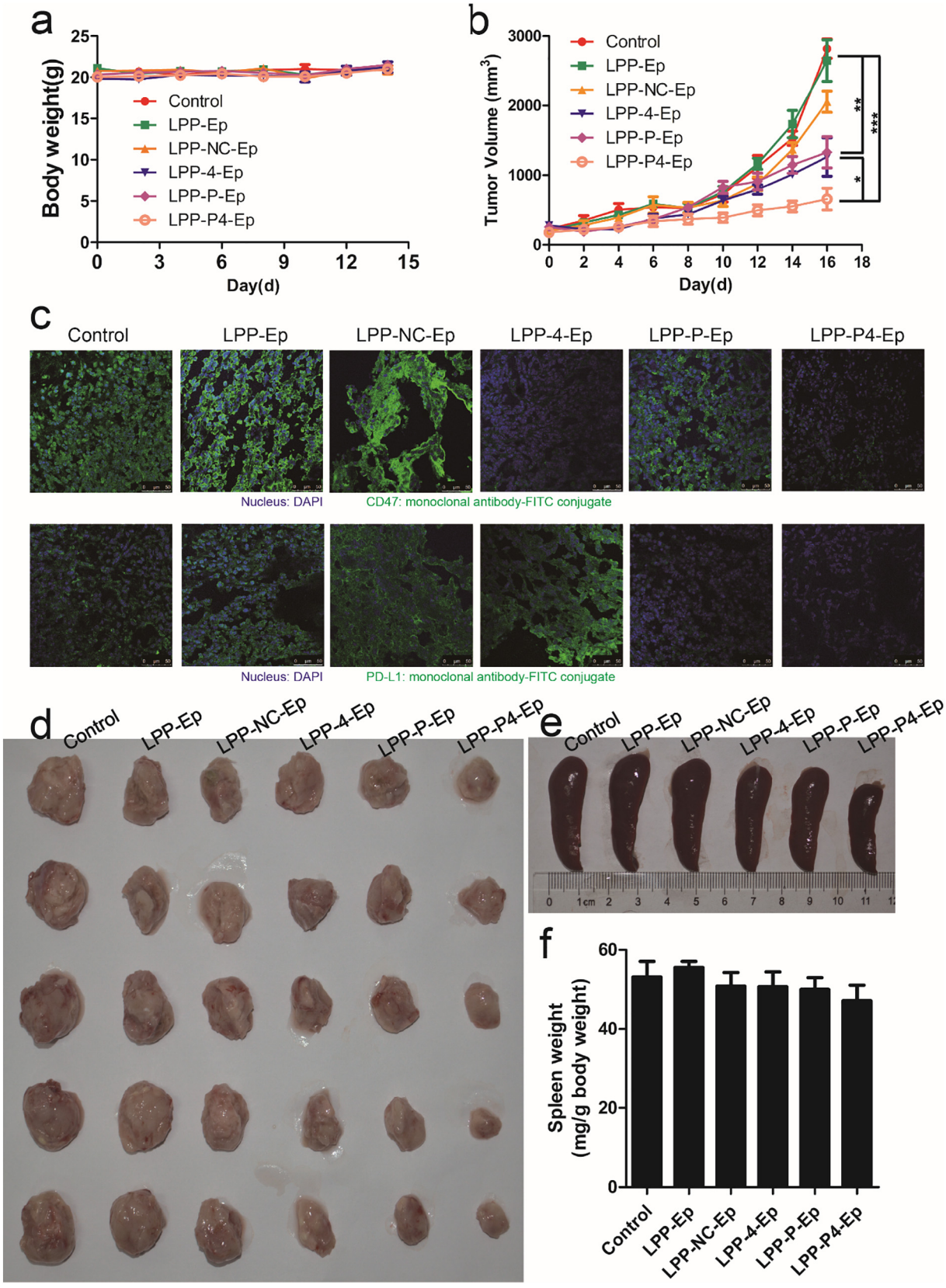

Fig. 5. In vivo antitumor effects of LPP-P4-Ep for solid tumor. (a) Mice weight changes. Each data point was represented as mean ± SEM. $n = 6$ (b) Tumor size changes of 4 T1 model mice after treated with PBS, LPP-Ep, LPP-NC-Ep, LPP-4-Ep, LPP-P-Ep and LPP-P4-Ep. $^{*}P < 0.05$, $^{**}P < 0.01$, $^{***}P < 0.001$ compared to the control group by ANOVA test (c) Immunofluorescence images of CD47 and PD-L1 on tumor tissue. The nucleus was stained with Hoechst 33258. (d) Collecting tumor tissue after administration. (e-f) The spleens were isolated and weighted, and spleen weight index were calculated as organ weight (milligram, mg) per gram (g) of mouse body weight. All error bars expressed as mean ± SEM ($n = 3$).

response that cellular immunity and cytokines secretion may further promote NK cell immune response and antibody production.

The H&E staining of heart, liver, spleen, lung, kidney and tumor was conducted to analyze the toxicity of LPP-Ep complexes in vivo. Significant metastases can be seen in each group lung tissue except LPP-P4-Ep group. Normal tissues, such as heart, liver, spleen, lung, kidney and tumor were shown in Fig. 7. Histological features of control group mouse showed normal structures. Moreover, main viscera tissues including heart, liver, spleen and kidney show no remarkable histopathological abnormalities or lesions in LPP-Ep treated group. However, compared to the other four therapeutic groups, the PBS and LPP-Ep group appeared much more hypercellular and meanwhile exhibited higher level of unclear polymorphism in H&E strained lung and tumor sections (Fig. 7b). Moreover, tumor tissue from the LPP-P4-Ep group showed the lowest cancer cell density.

3.5. Systemic delivery of LPP-NPs containing si-CD47 or si-PD-L1 to suppress tumor metastasis model

In order to evaluate whether the targeted delivery of si-CD47 and si-PD-L1 to cancer cells can be therapeutically applied to combat the homing of circulating cells in the lung, we used a well-established 4 T1 metastasis model, which spontaneously generated lung metastasis [35]. LPP-Ep containing CD47 or/and PD-L1 was injected into Balb/c animals every 3 days, 6 times (dose = 0.4 mg/kg) from 2 days after inoculation. As shown in Fig. 8a, there was no significant difference in body weight among six groups, indicating that tail vein injection of these liposome complexes was also safe and biocompatible with subcutaneous injection. And lung micro-metastasis was significantly lower in the LPP-P4-Ep group than in the untreated group or the LPP-P-Ep/LPP-4-Ep group. (Fig. 8b-c). The results demonstrated that LPP-P4-Ep could significantly decrease tumor metastasis, ~85% of that of the untreated control. The distributions of LPP-P4-Ep in tissues were detected in fluorescence signal of Cy5-EpCAM at 2, 4 and 12 h by fluorescence spectrophotometer (Fig. 8d) and confocal microscopy (Fig. 8e). The accumulation of LPP-P4-Ep in heart, liver, spleen, lung and kidney reached the maximum values at 4 h, and decreased significantly at 12 h, which may due to the metabolism in blood of mice. The results revealed that LPP-P4-Ep (red) were still accumulated in the lungs after 12 h.

The histological analysis of the lung tissues showed fewer and smaller lung micro-metastases observed in LPP-P4-Ep-treated animals, compared to the LPP-P-Ep-treated/ LPP-4-Ep-treated animals (Fig. 9a). H&E results were consistent with the metastasis number results. Checkpoints stimulation can change local cytokine microenvironment that will in turn influence the differentiation of T helpers, whose appropriate reaction is essential to the development and function of B cells. Therefore, we assessed the percentage of T cells, NK cells, NKT cells and the cytokine profile in mice blood. The cytokines in blood were determined

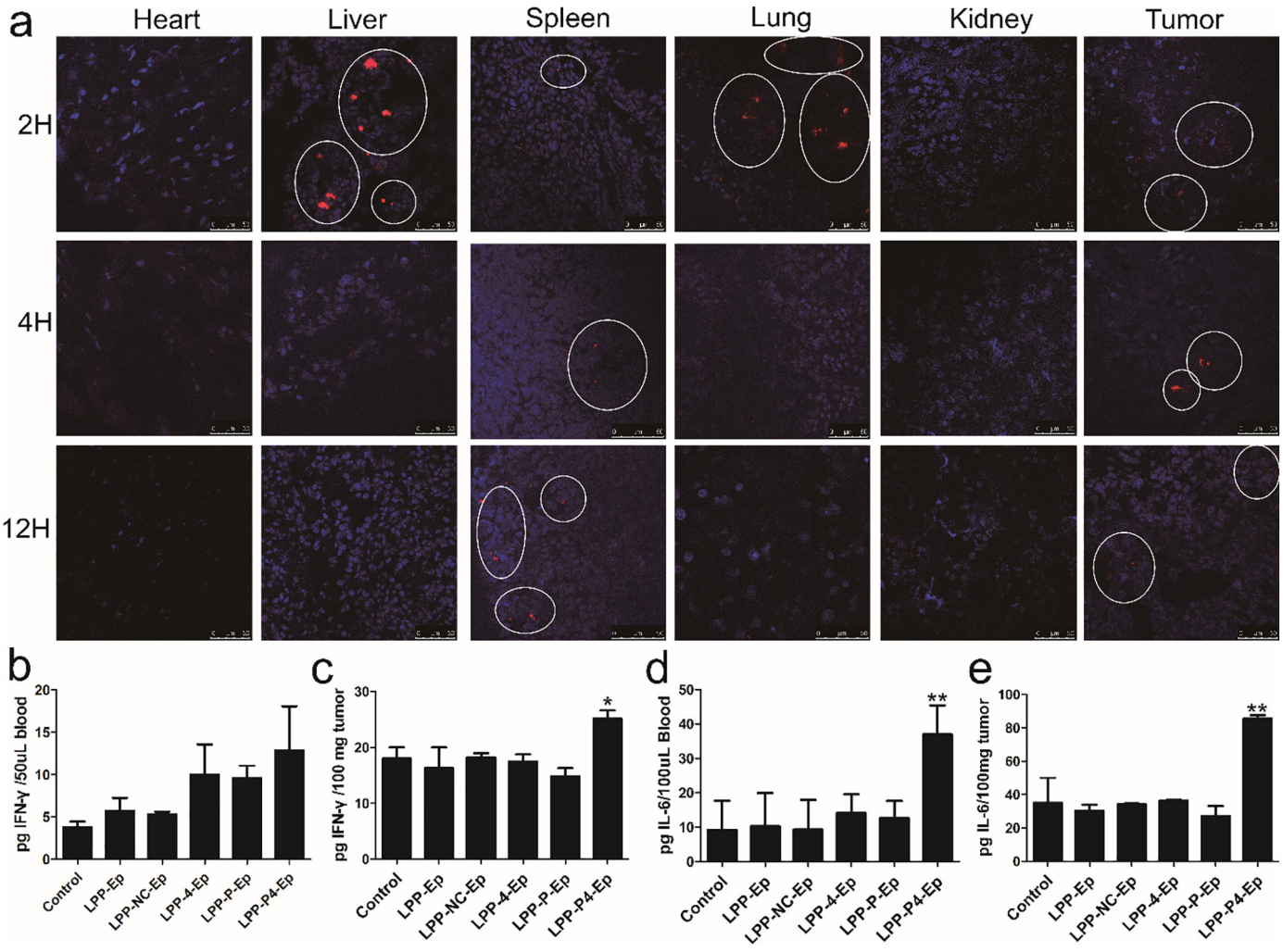

Fig. 6. LPP-P4-Ep distribution of 4 T1 model mice in tumor, heart, liver, spleen, lung and kidney. (a) Images of tumor, heart, liver, spleen, lung and kidney at 2, 4 and 12 h. Nuclei was stained by hoechst 33258 (blue) and Cy5-labelled LPP-Ep was red. (b-e) The levels of IFN-γ and IL-6 cytokines of mice in tumor and in blood were detected by ELISA. Data were expressed as mean ± SEM. $^{*}P < 0.05$, $^{**}P < 0.01$, $^{***}P < 0.001$ compared with the control group by ANOVA test.

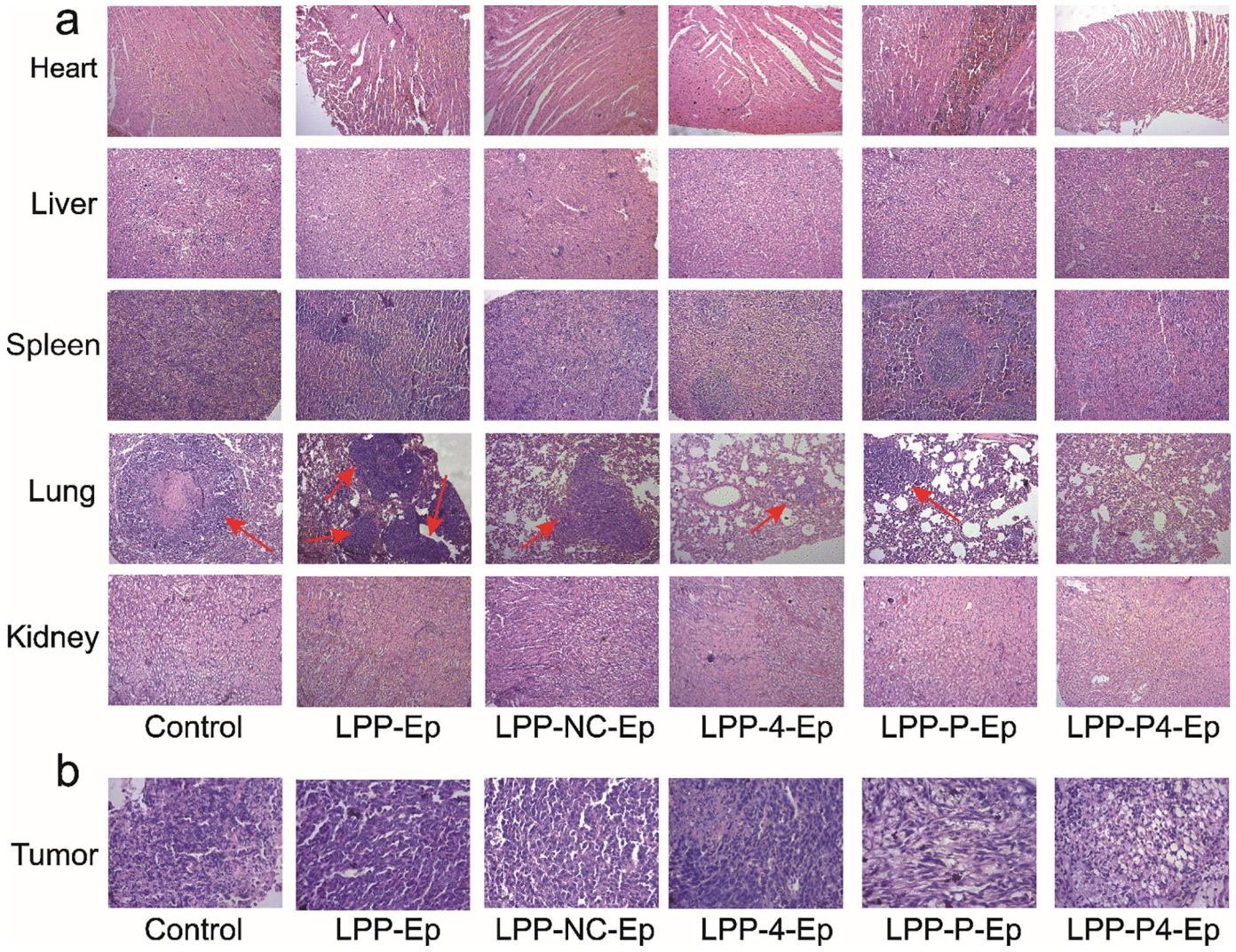

Fig. 7. The immunohistochemistry of heart, liver, spleen, lung, kidney and tumor. Nuclei were strained blue and cytoplasm was strained in red. (a) Immunohistochemistry of Heart, Liver, Spleen, Lung and Kidney collected from the endpoint from the endpoint of the experiment, amplification × 40. (b) Immunohistochemistry of tumor collected from the endpoint from the endpoint of the experiment, amplification × 100.

by CBA assay. The LPP-P4-Ep group mice maintained higher level in T cells (Fig. 9b) compared to the control, but among the six group the percentage of NK cells and NKT cells maintained the same levels (Fig. 9c-d). The LPP-P4-Ep group mice also contained significantly higher levels of immune cytokines including IL-10, IFN-γ, IL-4 and IL-6 than those of the PBS control mice (Fig. 9f-l), but no significant different in TNF, IL-17A and IL-2 cytokines. These results indicated that cellular immunity and cytokine secretion induced by blockade CD47 and PD-L1 would further promote T cell differentiation and mixed cytokines immune responses. The detection method of different cytokines was showed in Fig. 9e. The standard curve lines of IL-10, IFN-γ, TNF, IL-17A, IL-4, IL-1 and IL-6 were listed in Fig. S9.

3.6. Systemic delivery of si-CD47 or/and si-PD-L1 in LPP-Ep caused no anemia in blood

Systemic administration can cause a certain degree of side effects, and one of the primary goals of pharmaceutical science is to reduce undesirable side effects by improving the pharmacokinetic profile and biodistribution of the therapeutic agent. To evaluate whether systemic administration of si-CD47 or/and si-PD-L1 produced any side effects to circulating hematopoietic cells, a hematology examination was performed on the blood samples collected after animals receiving injections of LPP-P4-Ep for 6 injections. The WBC, HCT, PLT, RBC and HGB cell counts of LPP-P4-Ep treated mice were not significantly different from the control groups (Fig. 10). These results indicated that LPP-P4-Ep was the safety and effective gene delivery for the treatment of cancer.

4. Discussion

High invasiveness and metastasis of each kind of tumor requires the cells to be able to survive and evade immune system once they are detached from the immunosuppressive primary microenvironment and until they establish a metastatic site. PD-L1 is a transmembrane protein involved in the immune system suppression [36]. CD47 is a receptor that is ubiquitously expressed on cell surfaces; it conveys a "self" signal to the macrophages and T cells to limit clearance from the system [16,37]. CD47 and PD-L1 serve as critical innate and adaptive checkpoints, respectively, which are critical to the immune system. The expression of CD47 and PD-L1 was elevated in various cancer cells including lung cancer cells, breast cancer cells, melanoma cells [38] and esophageal cancer [39], bur except normal cells (Table 1). Si-CD47 and si-PD-L1 co-loaded LPP-P4-Ep complexes were modified by aptamer EpCAM (Figs. 1-2 and Fig.S1). The enhanced cancer targeting (Fig. 3), increased down-regulation of immune-related proteins

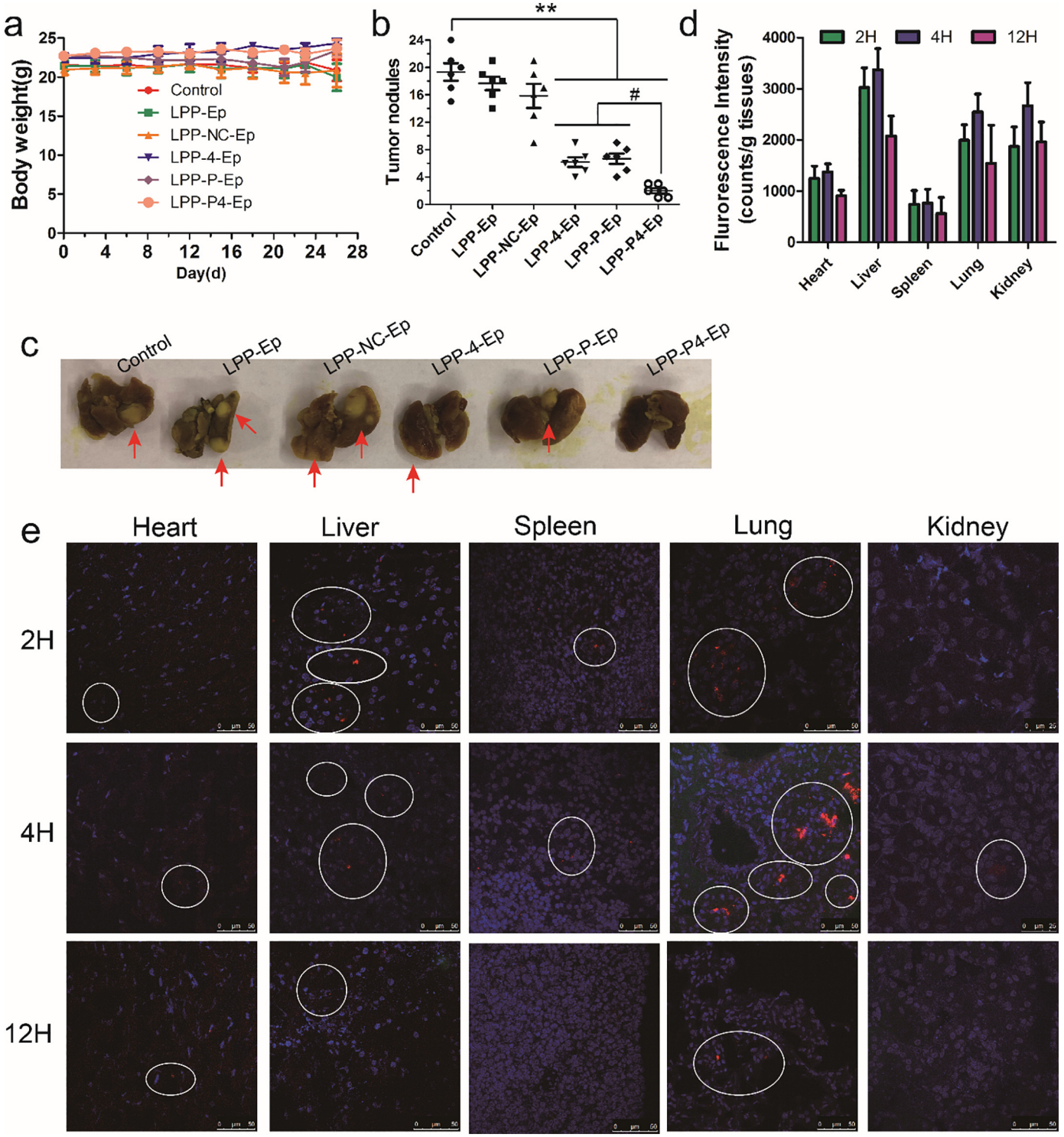

Fig. 8. In vivo antitumor effects of LPP-P4-Ep in lung metastasis. (a) Mice weight changes. Each data point was represented as mean ± SEM, $n = 6$. (b) 4 T1 tumor nodules in lungs of mice after treatment of nanoparticle complexes. Data were expressed as mean ± SEM. $^{*}P < 0.05$, $^{**}P < 0.01$, $^{***}P < 0.001$ compared with the control group by ANOVA test. $^{\#}P < 0.05$, $^{\#\#}P < 0.01$ compared with the LPP-P4-Ep group by ANOVA test. (c) The gross appearance of tumor nodules of 4T1 (shown in arrows) in lungs after fixation with Bouin's solution for 24 h. (d) LPP-P4-Ep distribution in heart, liver, spleen, lung and kidney at 2, 4 and 12 h. The error bars expressed as mean ± SEM ($n = 3$). (e) Confocal microscopic images of heart, liver, spleen, lung and kidney at 2, 4 and 12 h. Nuclei was stained by hoechst 33258 (blue) and Cy5-labelled LPP-Ep was red.

expression, and inducted cancer cells apoptosis with immune cells obviously demonstrated the effectiveness of LPP-P4-Ep in high CD47 and PD-L1 expression immune evasion cells (Fig. 4). In Fig. 4, the CD47 and PD-L1 proteins inhibition by siRNA are small, but there are statistical differences among each group. After incubating CD47-inhibited and PD-L1-inhibited cells with monocyte cells, IFN-γ and IL-6 secreted by monocyte cells were highest (Fig. S4), which are critical to CD47/SIPR-α [40] and PD-L1/PD-1 [41] axis immune response.

In vitro data demonstrated that inhibition of CD47 and PD-L1 proteins induced immune cell activation and cytokine secretion, and decreased tumor growth and tumor metastasis. This reduction was observed in 4 T1 subcutaneous models (Figs. 5-7 and Figs. S6-7) and

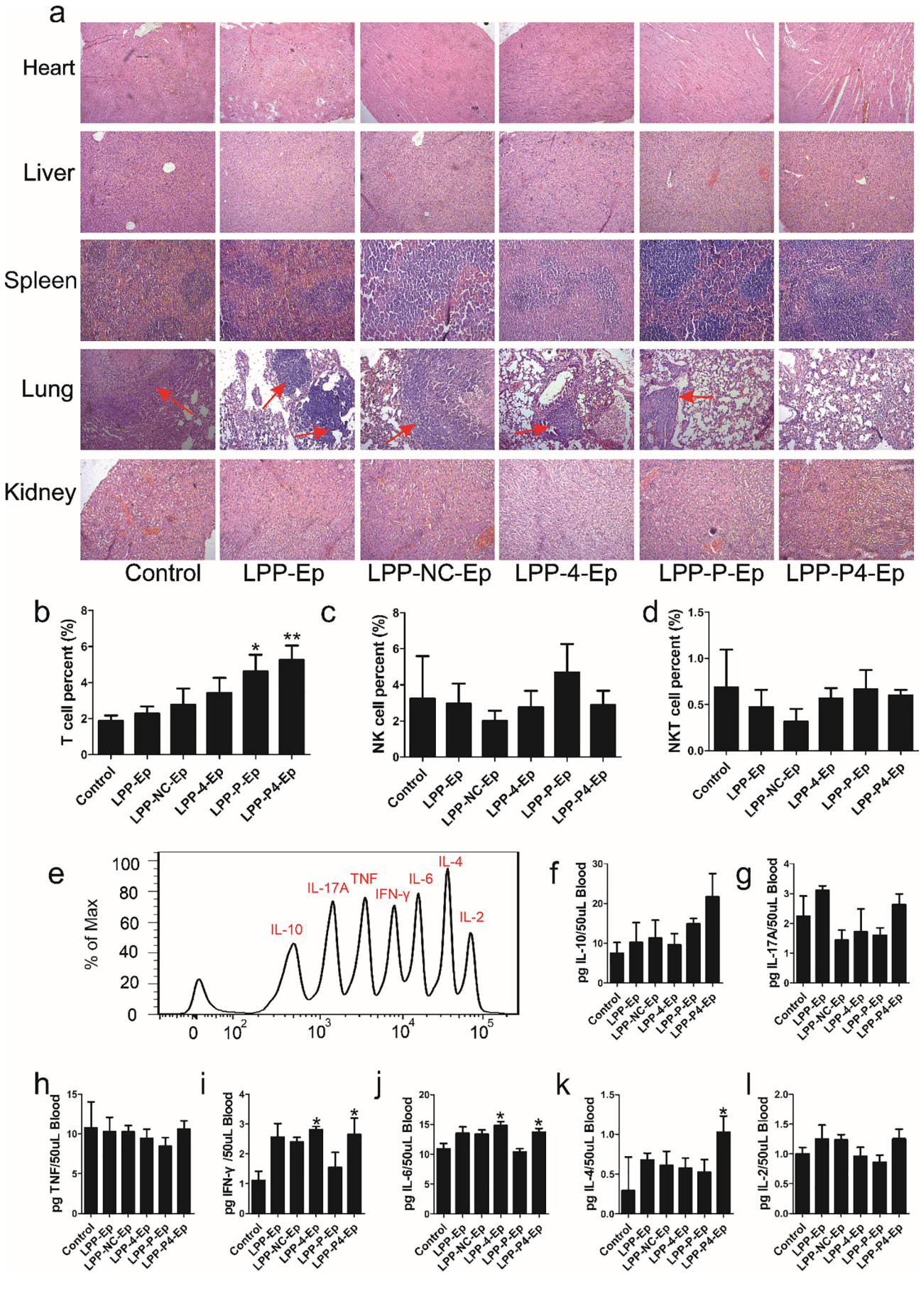
a
Heart
Liver
Spleen
Lung
Kidney
Control
LPP-Ep
LPP-NC-Ep
LPP-4-Ep
LPP-P-Ep
LPP-P4-Ep
b
T cell percent (%)
c
NK cell percent (%)
d
NKT cell percent (%)
e
% of Max
IL-10
IL-17A
TNF
IFN-γ
IL-6
IL-4
IL-2
f
pg IL-10/50uL Blood
g
pg IL-17A/50uL Blood
h
pg TNF/50uL Blood
i
pg IFN-γ /50uL Blood
j
pg IL-6/50uL Blood
k
pg IL-4/50uL Blood
l
pg IL-2/50uL Blood

Fig. 9. The immunohistochemistry and CBA assay. (a) Immunohistochemistry of heart, liver, spleen, lung and kidney collected from the endpoint from the endpoint of the experiment, amplification × 40. (b-d) The percent of T cells, NK cells and NKT cells in leukocyte after nanoparticle complexes treatment ten days. $^{*}P < 0.05$, $^{**}P < 0.01$, $^{***}P < 0.001$ compared to the control group by ANOVA test. (e-l) The levels of cytokines including IFN-γ, IL-17A, TNF, IL-2, IL-4, IL-6 and IL-10 in sera of immunized mice were detected by quantitative CBA. $^{*}P < 0.05$, $^{**}P < 0.01$, $^{***}P < 0.001$ compared to the control group by ANOVA test. All error bars expressed as mean ± SEM (n = 3).

4 T1 metastasis models (Fig. 8), when the immune-associated proteins were blocked by injection of LPP-PE-Ep. After injected with LPP-P4-Ep, in subcutaneous models IFN-γ and IL-6 on mice blood and tumors were significant higher. And in metastasis model (Fig. 9) the secretion of IL-10, IFN-γ, IL-6 and IL-4 cytokines on blood were higher, too. These cytokines IL-10, IFN-γ, IL-6 and IL-4 are critical to immune response, specially IFN-γ is essential for anti-tumor response, stimulates the development of cytotoxic T lymphocytes, improves antigen presentation and many more [42].

Interestingly, there are few reports on the simultaneous targeting of CD47 and PD-L1, and most of the physiological activity on CD47 or PD-L1 is studied by using monoclonal antibodies, which was just mechanically injected into the body. The LPP-Eps accumulated in the proximity of the cancer cells (Figs. 6a and 8d-e), prolonged half-life and controlled the tropism of therapeutics [43]. In our research, even though repeated injections of the LPP-Ep loading si-CD47 or/and si-PD-L1 effectively inhibited tumor growth while maintaining blood parameters even after 6 administrations (Fig. 10).

Our study has revealed the critical coordination of tumor-cell-relation CD47 and PD-L1 for tumor evasion. Based on this finding, we have developed EpCAM-targeted LPP-Ep complexes that simultaneously decrease both CD47 and PD-L1 proteins on tumor cells, while reducing their off-target binding to healthy cells. The strategy results in significantly showed the enhanced anti-tumor effects in both CD47 and PD-L1 inhibition compared to either CD47 or PD-L1 inhibition alone. Synergistic effects of CD47 and PD-L1 were only reported in recent years using antibody therapies [17,18]. Balb/c mice repeatedly injected with LPP-P4-Ep containing si-CD47 and si-PD-L1 did not cause anemia effect. This might be expected because aptamer EpCAM-modified LPP-Ep can selectively target to tumor cells and PEGylated complexes can reduce uptake of nanoparticles by leukocytes [44]. The major concern regarding the antibody therapy was solved by utilization the LPP-Ep nanoparticle formulation to avoid side effects. CD47 and PD-L1 serve as critical innate and adaptive checkpoints, respectively, both of them are critical to the immune system. Therefore, we believe this dual-targeting strategy will provide insight into tumor immunotherapy for better tumor control. Meanwhile, LPP-Ep formulation could be a versatile platform that co-deliver gene/drugs/chemo into individual cancer cells to target multiple signaling pathways.

Acknowledgments

This research was supported by the Ministry of Science and Technology of the People's Republic of China (grant number 2015CB931804); the National Natural Science Foundation of China (NSFC, grant numbers 81703555, U1505225 and 81773063), and the China Postdoctoral Science Foundation (grant number 2017M620268).

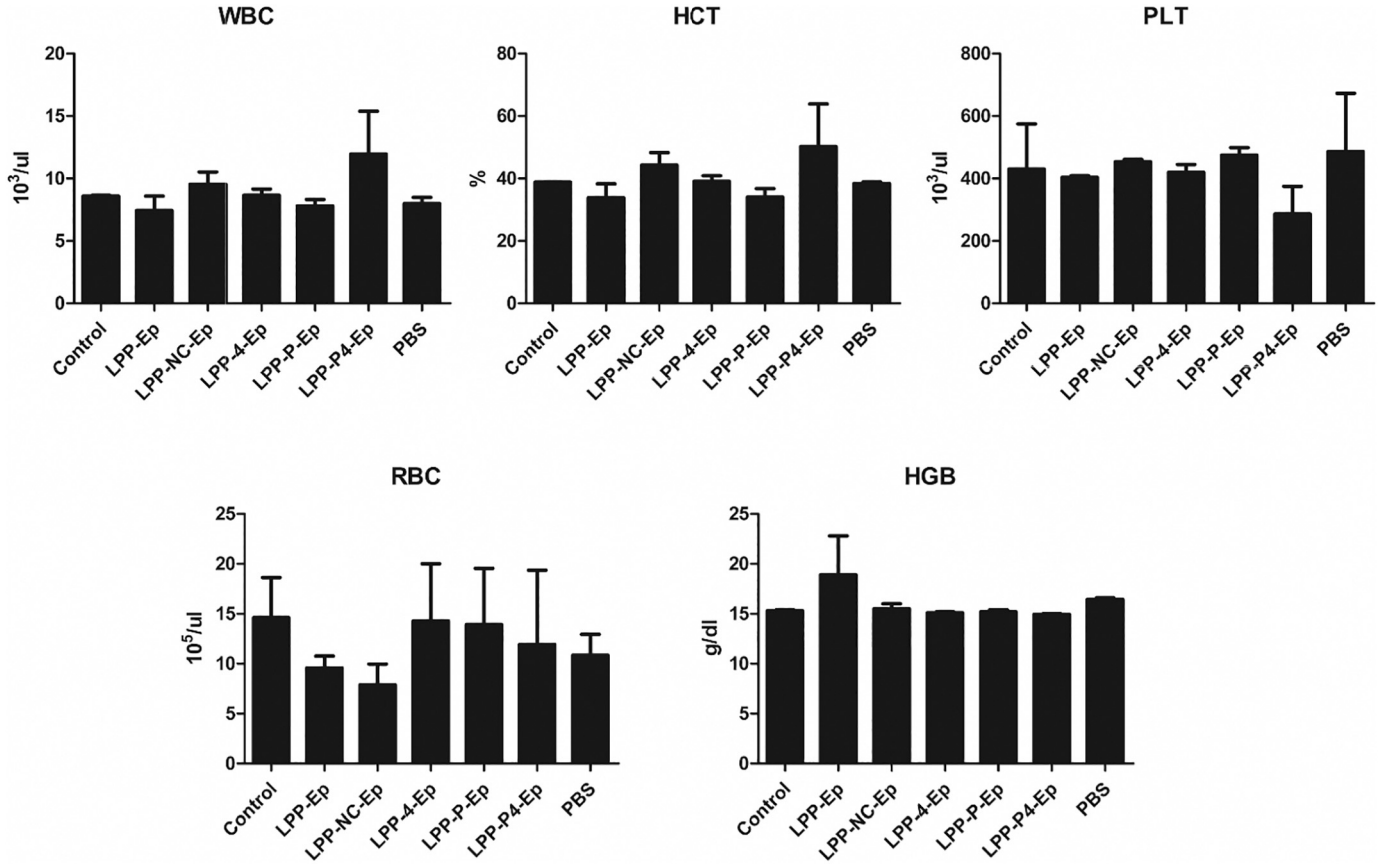

Fig. 10. LPP-P4-Ep caused no anemia. Whole blood analysis about hematology collected from Babl/c mice treated with LPP-P4-Ep loading anti-CD47 or anti-PD-L1 siRNA ($n = 5$). HCT, hematocrit; HGB, hemoglobin; PLT, platelet; RBC, red blood cell; WBC, white blood cell. $^{*}P < 0.05$ compared to the control group by ANOVA test. All error bars expressed as mean ± SEM (n = 3).

Author contributions

S.L. and Y.L. conceived and designed the experiments. S.L., R.X., Y.Y., X.X., Y. C., B. L. and S.L. performed the experiments. S.L. and X.X. acquired and analyzed the experimental data. S.L., X.X. and L. J. wrote the manuscript. All authors reviewed the manuscript.

Competing Interests

The authors declare no competing interests.

Appendix A. Supplementary data

Supplementary data to this article can be found online at https://doi.org/10.1016/j.ebiom.2019.03.018.

References

[1] Mellman I, Coukos G, Dranoff G. Cancer immunotherapy comes of age. Nature 2011;480:480–9. https://doi.org/10.1038/nature10673.
[2] Zhu EF, et al. Synergistic innate and adaptive immune response to combination immunotherapy with anti-tumor antigen antibodies and extended serum half-life IL-2. Cancer Cell 2015;27:489–501. https://doi.org/10.1016/j.ccell.2015.03.004.
[3] Park S, et al. The therapeutic effect of anti-HER2/neu antibody depends on both innate and adaptive immunity. Cancer Cell 2010;18:160–70. https://doi.org/10.1016/j.ccr.2010.06.014.
[4] Yang X, et al. Cetuximab-mediated tumor regression depends on innate and adaptive immune responses. Mol Ther 2013;21:91–100.
[5] Dong H, et al. Tumor-associated B7-H1 promotes T-cell apoptosis: a potential mechanism of immune evasion. Nat Med 2002;8:793–800. https://doi.org/10.1038/nm730.
[6] Thompson RH, et al. Costimulatory B7-H1 in renal cell carcinoma patients: Indicator of tumor aggressiveness and potential therapeutic target. Proc Natl Acad Sci U S A 2004;101:17174–9. https://doi.org/10.1073/pnas.0406351101.
[7] Shih K, Arkenau HT, Infante JR. Clinical impact of checkpoint inhibitors as novel cancer therapies. Drugs 2014;74:1993–2013. https://doi.org/10.1007/s40265-014-0305-6.
[8] Palucka K, Banchereau J. Cancer immunotherapy via dendritic cells. Nat Rev Cancer 2012;12:265–77. https://doi.org/10.1038/nrc3258.
[9] Melero I, et al. Evolving synergistic combinations of targeted immunotherapies to combat cancer. Nat Rev Cancer 2015;15:457–72. https://doi.org/10.1038/nrc3973.
[10] Brown EJ, Frazier WA. Integrin-associated protein (CD47) and its ligands. Trends Cell Biol 2001;11:130–5.
[11] Brown E, Hooper L, Ho T, Gresham H. Integrin-associated protein: a 50-kD plasma membrane antigen physically and functionally associated with integrins. J Cell Biol 1990;111:2785–94.
[12] Lindberg FP, Gresham HD, Schwarz E, Brown EJ. Molecular cloning of integrin-associated protein: an immunoglobulin family member with multiple membrane-spanning domains implicated in alpha v beta 3-dependent ligand binding. J Cell Biol 1993;123:485–96.
[13] Wang XQ, Frazier WA. The thrombospondin receptor CD47 (IAP) modulates and associates with alpha2 beta1 integrin in vascular smooth muscle cells. Mol Biol Cell 1998;9:865–74.
[14] Ho CC, et al. Velcro engineering of high affinity CD47 ectodomain as signal regulatory protein alpha (SIRPalpha) antagonists that enhance antibody-dependent cellular phagocytosis. J Biol Chem 2015;290:12650–63. https://doi.org/10.1074/jbc.M115.648220.
[15] Barclay AN, Van den Berg TK. The interaction between signal regulatory protein alpha (SIRPalpha) and CD47: structure, function, and therapeutic target. Annu Rev Immunol 2014;32:25–50. https://doi.org/10.1146/annurev-immunol-032713-120142.
[16] Liu X, Kwon H, Li Z, Fu YX. Is CD47 an innate immune checkpoint for tumor evasion. J Hematol Oncol 2017;10:12. https://doi.org/10.1186/s13045-016-0381-z.
[17] Sockolosky JT, et al. Durable antitumor responses to CD47 blockade require adaptive immune stimulation. Proc Natl Acad Sci U S A 2016;113:E2646–54. https://doi.org/10.1073/pnas.1604268113.
[18] Liu X, et al. Dual targeting of innate and adaptive checkpoints on tumor cells limits immune evasion. Cell Rep 2018;24:2101–11. https://doi.org/10.1016/j.celrep.2018.07.062.
[19] Dheilly E, et al. Selective blockade of the ubiquitous checkpoint receptor CD47 is enabled by dual-targeting Bispecific antibodies. Mol Ther 2017;25:523–33. https://doi.org/10.1016/j.ymthe.2016.11.006.
[20] Cheng J, et al. Formulation of functionalized PLGA-PEG nanoparticles for in vivo targeted drug delivery. Biomaterials 2007;28:869–76. https://doi.org/10.1016/j.biomaterials.2006.09.047.
[21] Casey SC, et al. MYC regulates the antitumor immune response through CD47 and PD-L1. Science 2016;352:227–31. https://doi.org/10.1126/science.aac9935.
[22] Gao H, et al. Precise glioma targeting of and penetration by aptamer and peptide dual-functioned nanoparticles. Biomaterials 2012;33:5115–23. https://doi.org/10.1016/j.biomaterials.2012.03.058.
[23] Allen TM, Brandeis E, Hansen CB, Kao GY, Zalipsky S. A new strategy for attachment of antibodies to sterically stabilized liposomes resulting in efficient targeting to cancer cells. Biochim Biophys Acta 1995;1237:99–108.
[24] Igarashi S, Hattori Y, Maitani Y. Biosurfactant MEL-A enhances cellular association and gene transfection by cationic liposome. J Controll Release 2006;112:362–8. https://doi.org/10.1016/j.jconrel.2006.03.003.
[25] Dai Y, et al. Liposomes containing bile salts as novel ocular delivery systems for tacrolimus (FK506): in vitro characterization and improved corneal permeation. Int J Nanomed 2013;8:1921–33. https://doi.org/10.2147/IJN.S44487.
[26] Li L, et al. Nucleolin-targeting liposomes guided by aptamer AS1411 for the delivery of siRNA for the treatment of malignant melanomas. Biomaterials 2014;35:3840–50. https://doi.org/10.1016/j.biomaterials.2014.01.019.
[27] Gao J, et al. The promotion of siRNA delivery to breast cancer overexpressing epidermal growth factor receptor through anti-EGFR antibody conjugation by immunoliposomes. Biomaterials 2011;32:3459–70. https://doi.org/10.1016/j.biomaterials.2011.01.034.
[28] Su S, et al. CRISPR-Cas9-mediated disruption of PD-1 on human T cells for adoptive cellular therapies of EBV positive gastric cancer. Oncoimmunology 2017;6:e1249558. https://doi.org/10.1080/2162402X.2016.1249558.
[29] Belz GT, et al. The CD8alpha(+) dendritic cell is responsible for inducing peripheral self-tolerance to tissue-associated antigens. J Exp Med 2002;196:1099–104.
[30] Cheng Y, et al. Metastatic cancer cells compensate for low energy supplies in hostile microenvironments with bioenergetic adaptation and metabolic reprogramming. Int J Oncol 2018;53:2590–604. https://doi.org/10.3892/ijo.2018.4582.
[31] Lian S, et al. S-nitrosocaptopril interrupts adhesion of cancer cells to vascular endothelium by suppressing cell adhesion molecules via inhibition of the NF-small ka, CyrillicB and JAK/STAT signal pathways in endothelial cells. Eur J Pharmacol 2016;791:62–71. https://doi.org/10.1016/j.ejphar.2016.08.018.
[32] Fischer D, Li Y, Ahlemeyer B, Krieglstein J, Kissel T. In vitro cytotoxicity testing of polycations: influence of polymer structure on cell viability and hemolysis. Biomaterials 2003;24:1121–31.
[33] Emmert MY, et al. Human stem cell-based three-dimensional microtissues for advanced cardiac cell therapies. Biomaterials 2013;34:6339–54. https://doi.org/10.1016/j.biomaterials.2013.04.034.
[34] Chono S, Li SD, Conwell CC, Huang L. An efficient and low immunostimulatory nanoparticle formulation for systemic siRNA delivery to the tumor. J Controll Release 2008;131:64–9. https://doi.org/10.1016/j.jconrel.2008.07.006.
[35] Tang Q, et al. A novel co-drug of aspirin and ursolic acid interrupts adhesion, invasion and migration of cancer cells to vascular endothelium via regulating EMT and EGFR-mediated signaling pathways: multiple targets for cancer metastasis prevention and treatment. Oncotarget 2016;7:73114–29. https://doi.org/10.18632/oncotarget.12232.
[36] Zhao Y, et al. Antigen-presenting cell-intrinsic PD-1 neutralizes PD-L1 in cis to attenuate PD-1 Signaling in T cells. Cell Rep 2018;24. https://doi.org/10.1016/j.celrep.2018.06.054 379-390 e376.
[37] Weiskopf K. Cancer immunotherapy targeting the CD47/SIRPalpha axis. Eur J Cancer 2017;76:100–9. https://doi.org/10.1016/j.ejca.2017.02.013.
[38] Cerezo M, et al. Translational control of tumor immune escape via the eIF4F-STAT1-PD-L1 axis in melanoma. Nat Med 2018. https://doi.org/10.1038/s41591-018-0217-1.
[39] Zhao CL, et al. Characterization of cluster of differentiation 47 expression and its potential as a therapeutic target in esophageal squamous cell cancer. Oncol Lett 2018;15:2017–23. https://doi.org/10.3892/ol.2017.7447.
[40] Fidyk W, et al. Evaluation of proinflammatory and immunosuppressive cytokines in blood and bone marrow of healthy hematopoietic stem cell donors. Cytokine 2018;102:181–6. https://doi.org/10.1016/j.cyto.2017.09.001.
[41] Pardoll DM. The blockade of immune checkpoints in cancer immunotherapy. Nat Rev Cancer 2012;12:252–64. https://doi.org/10.1038/nrc3239.
[42] Yang YG, Wang H, Asavaroengchai W, Dey BR. Role of interferon-gamma in GVHD and GVL. Cell Mol Immunol 2005;2:323–9.
[43] Matsumura Y, Maeda H. A new concept for macromolecular therapeutics in cancer chemotherapy: mechanism of tumoritropic accumulation of proteins and the antitumor agent smancs. Cancer Res 1986;46:6387–92.
[44] Gref R, et al. Biodegradable long-circulating polymeric nanospheres. Science 1994;263:1600–3.